

Discordances in Cosmology and the Violation of Slow-Roll Inflationary Dynamics

Akhil Antony^{✉*}

*The Institute of Mathematical Sciences, HBNI, CIT Campus, Chennai 600113, India
and Homi Bhabha National Institute, Training School Complex, Anushakti Nagar, Mumbai 400085, India*

Fabio Finelli[†]


*INAF/OAS Bologna, Osservatorio di Astrofisica e Scienza dello Spazio,
Area della ricerca CNR-INAF, via Gobetti 101, I-40129 Bologna, Italy
and INFN, Sezione di Bologna, via Irnerio 46, 40126 Bologna, Italy*

Dhiraj Kumar Hazra[‡]

*The Institute of Mathematical Sciences, HBNI, CIT Campus, Chennai 600113, India;
Homi Bhabha National Institute, Training School Complex, Anushakti Nagar, Mumbai 400085, India;
and INAF/OAS Bologna, Osservatorio di Astrofisica e Scienza dello Spazio,
Area della ricerca CNR-INAF, via Gobetti 101, I-40129 Bologna, Italy*

Arman Shafieloo[§]

*Korea Astronomy and Space Science Institute, Daejeon 34055, Korea
and University of Science and Technology, Daejeon 34113, Korea*

 (Received 25 March 2022; revised 24 May 2022; accepted 9 February 2023; published 13 March 2023)

We identify examples of single field inflationary trajectories beyond the slow-roll regime that improve the fit to Planck 2018 data compared to a baseline Λ cold dark matter model with power law form of primordial spectrum and at the same time alleviate existing tensions between different datasets in the estimate of cosmological parameters such as H_0 and S_8 . A damped oscillation in the first Hubble flow function—or equivalently a feature in the potential—and the corresponding localized oscillations in the primordial power spectrum partially mimic the improvement in the fit of Planck data due to A_L or Ω_K . Compared to the baseline model, this model can lead *simultaneously* to a larger value of H_0 and a smaller value of S_8 , a trend that can be enhanced when the most recent SH0ES measurement for H_0 is combined with Planck and BICEP-Keck 2018 data. Large scale structure data and more precise cosmic microwave background polarization measurements will further provide critical tests of this intermediate fast-roll phase.

DOI: [10.1103/PhysRevLett.130.111001](https://doi.org/10.1103/PhysRevLett.130.111001)

Introduction.—Thanks to the precise measurement of the cosmic microwave background (CMB) anisotropy pattern, cosmology has entered a precision era. Although Λ cold dark matter (Λ CDM) is still theoretically incomplete in terms of the fundamental constituents of dark matter and dark energy, new physics beyond the six parameters of the flat Λ CDM concordance cosmology have not emerged yet within Planck 2018 (P18) data [1,2]. Among the so-called “anomalies,” P18 temperature data seem to indicate an extra smoothing of the acoustic peaks at multipoles higher than 800 and a low amplitude at multipoles lower than 40 with respect to what Λ CDM predicts. These effects are the main reason why a phenomenological rescaling of the lensing amplitude A_L or a positive spatial curvature Ω_K [1] improve the fit for P18 temperature and polarization data at nearly 3σ , although the stretches in these parameters are reduced when P18 CMB lensing is included in the analysis.

Two theoretical explanations for this extra smoothing, such as compensated CDM isocurvature perturbations and

primordial features, were proposed in [2]. The latter consisted of an analytical template for superimposed oscillations linear in the wave number with a Gaussian envelope, similar to the form that can mimic CMB lensing obtained earlier in the blind reconstruction [3], that can mimic the smoothing of the acoustic peaks in a similar way to A_L for temperature anisotropies; whereas the amplitude of compensated CDM isocurvature was drastically reduced when the P18 CMB lensing was added [2]. Reconstruction and analytical templates of primordial features mimicking A_L were further studied in [4].

In this Letter, we connect inflationary dynamics beyond slow roll to the localized superimposed oscillations that provide an improved fit to P18 data by employing a profile in the Hubble parameter during inflation. Equipped with this theoretical proposal, we then study how these particular types of localized features possibly hidden in P18 data lead simultaneously to a larger H_0 and a lower S_8 and, therefore, potentially alleviate existing tensions of CMB data with

Cepheid calibrated type-Ia supernova [5], galaxy clustering, and weak lensing data [6,7]. Other proposals to increase H_0 , such as early dark energy [8] or some model of scalar-tensor gravity [9] (see Refs. [10,11] for reviews), also increase S_8 that worsen the tension with galaxy weak lensing data. Our Letter represents the first inflationary solution leading simultaneously to higher H_0 and lower S_8 . We also derive the class of inflaton potential from the Hubble parameter as new theoretical models of concordance.

Model, methodology, data, and analysis.—In order to reconstruct the Hubble flow parameters, we assume a baseline parametrization in terms of the number of e -folds N during inflation,

$$\epsilon_H^{\text{baseline}}(N) = \epsilon_1 \exp[\epsilon_2(N - N_*)]. \quad (1)$$

N_* is chosen as the e -fold at which the pivot scale 0.05 Mpc^{-1} crosses the Hubble radius. In this parametrization, we obtain the spectral tilt as $n_s \simeq 1 - 2\epsilon_1 - \epsilon_2$ and the tensor-to-scalar ratio as $r \simeq 16\epsilon_1$. This correspondence allows uncertainties on n_s and r similar to those obtained by sampling directly on physical parameters (see Refs. [12,13] for an analogous result also by taking into account the running). We now introduce an intermediate fast-roll phase. The fast-roll phase proposed here is modeled by localized sinusoidal oscillations in the Hubble parameter,

$$\epsilon_H(N) = \epsilon_H^{\text{baseline}}(N) \left(1 + \frac{\alpha \cos[\omega(N - N_0)]}{1 + \beta(N - N_0)^2} \right). \quad (2)$$

The damping of these oscillations linear in N with frequency ω is regulated by β . When $\beta \rightarrow 0$, this evolution generates resonant features [14–17] in the primordial power spectrum (PPS), while for $\omega \rightarrow 0$ we obtain sharp features [18–24]. In this general form, this flow function generates an envelope of $\sin + \sin \log + \sin$ oscillations where, at $N \rightarrow N_0$, the $\sin \log$ part is dominant (similar to [25]).

For the inflationary dynamics defined by Eqs. (1) and (2), we numerically solve for the Hubble parameter and for the scalar and tensor equations using Bunch-Davies vacuum initial conditions. For baseline analysis, we have three free parameters in the perturbation sector, namely, H^2/ϵ_1 , ϵ_1 , and ϵ_2 , which correspond to the scalar amplitude, scalar tilt, and tensor-to-scalar ratio [26]. When Eq. (2) is used for inflationary dynamics, we allow the fast-roll parameters to vary alongside the baseline parameters. Since there exist internal degeneracies within the fast-roll parameters, we vary α , ω , and N_0 and we fix $\log_{10} \beta = 2.5$. Note that fixing this parameter does not change the significance of the results noticeably [26].

We modified BINGO [27] to incorporate the Hubble flow function (HFF) instead of inflationary potential and use it as

an add on to CAMB [28]. In order to capture the entire primordial feature in the angular power spectrum, we compute the angular power spectrum at every multipole avoiding interpolation. CosmoMC [29] is used for parameter significance estimation.

In terms of CMB data, we use the P18 [30] and BICEP-Keck 2018 [31] likelihoods. We use four P18 dataset combinations, i.e., TT + low l + low E + BK18 (denoted as P18TT + BK18), TTTEEE + low l + low E + BK18 (P18TP + BK18), TTTEEE + low l + low E + lensing + BK18 (P18TPL + BK18), and TEEE + low l + low E + BK18 (P18TEEE + BK18). We use Planck Plik binned high- ℓ TT, TEEE, and TTTEEE datasets, since the features that help in resolving the concordance problem do not have very high-frequency oscillations [4] (in certain cases, we have also tested our models with unbinned Plik datasets and found nearly identical results). We allow all the foreground and calibration parameters corresponding to the datasets to vary as fast parameters. We also use the recently released H_0 measurement from SH0ES [5] (denoted as S21) with the above four data combinations separately.

Results.—The best-fit PPS obtained with BOBYQA [32] for baseline and for the model with fast roll are plotted in Fig. 1. In Table I, we tabulate the main results of our analysis for the eight data combinations. Our model provides 11 improvement in P18TP fit (in terms of χ^2) to the data with respect to the baseline. Most of the improvement (8.3) comes from the P18TT data, but a contribution to the improvement comes also from polarization data, as our results with TEEE show. The features in the PPS, introduced by the brief fast-roll phase are located mainly between $k \sim 0.1$ and 0.2 Mpc^{-1} , close to the largest multipoles probed by Planck. These oscillations are similar to superimposed oscillations with a Gaussian envelope [2] (bottom left panel of Fig. 1) and to the exact reconstruction of the one spectrum PPS (top left panel of Fig. 1) that mimics A_L discussed in [4]. The improvement in the fit

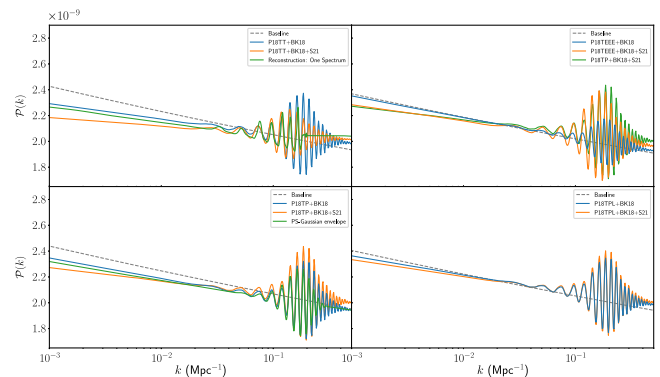


FIG. 1. Best-fit power spectra (PS) compared with the corresponding baseline ones for the same dataset combinations. The reconstructed “one spectrum” from [4] is plotted in the top left panel and the best-fit spectrum for superimposed oscillations with a Gaussian envelope [2] to P18TP is plotted in the bottom left.

TABLE I. Results from eight major data combinations from our analysis. $\Delta\chi^2$ values and their breakdown are quoted with respect to the baseline best fits. We also provide the marginalized confidence limits (C.L.) of the α parameter (in percent) deviating from the baseline $\alpha = 0$ value. The results for baseline are plotted in the top row of each data combination, while the results corresponding to Eq. (2) are plotted at the bottom cells. Bounds on n_s and r are provided using the HFFs assuming first-order approximation. In all cases, the two sided bounds represent 68% C.L. and upper bounds [as in the case of $16e_1 (\simeq r)$] represent 95% C.L. Without the addition of H_0 priors, the mean value of H_0 increases and S_8 and Ω_m decreases with fast roll.

Data	$\Delta\chi^2$			C.L.	$1 - 2e_1 - e_2 (\simeq n_s)$	$16e_1 (\simeq r)$	H_0	S_8	Ω_m
	Total	CMB	SHOES						
P18TT + BK18	-8.3	-8.3	...	82.7	0.963 ± 0.005 0.971 ± 0.007	< 0.036 < 0.040	66.86 ± 0.86 68.06 ± 1.14	0.840 ± 0.022 0.814 ± 0.027	0.321 ± 0.012 0.306 ± 0.015
P18TEEE + BK18	-2.7	-2.7	...	< 68	0.969 ± 0.009 0.968 ± 0.009	< 0.041 < 0.041	67.91 ± 0.77 67.63 ± 0.86	0.814 ± 0.020 0.819 ± 0.022	0.308 ± 0.010 0.311 ± 0.012
P18TP + BK18	-10.7	-10.7	...	72.5	0.965 ± 0.004 0.969 ± 0.005	< 0.036 < 0.037	67.26 ± 0.59 67.71 ± 0.66	0.835 ± 0.015 0.826 ± 0.017	0.317 ± 0.008 0.311 ± 0.009
P18TPL + BK18	-8.4	-8.4	...	70	0.965 ± 0.004 0.968 ± 0.004	< 0.035 < 0.037	67.35 ± 0.53 67.63 ± 0.57	0.832 ± 0.012 0.829 ± 0.013	0.315 ± 0.007 0.312 ± 0.008
P18TT + BK18 + S21	-19.5	-10.9	-8.6	> 99.9	0.976 ± 0.005 0.986 ± 0.007	< 0.040 < 0.047	69.41 ± 0.68 70.85 ± 0.78	0.781 ± 0.017 0.754 ± 0.018	0.287 ± 0.008 0.273 ± 0.008
P18TEEE + BK18 + S21	-1.2	-1.0	-0.2	< 68	0.981 ± 0.008 0.979 ± 0.009	< 0.046 < 0.040	69.76 ± 0.63 69.77 ± 0.67	0.772 ± 0.016 0.771 ± 0.017	0.284 ± 0.007 0.284 ± 0.008
P18TP + BK18 + S21	-19.3	-9.7	-9.6	98.6	0.973 ± 0.004 0.978 ± 0.004	< 0.039 < 0.041	68.71 ± 0.53 69.27 ± 0.58	0.802 ± 0.014 0.791 ± 0.014	0.297 ± 0.007 0.291 ± 0.007
P18TPL + BK18 + S21	-11.5	-10.4	-1.1	92.1	0.972 ± 0.004 0.975 ± 0.004	< 0.038 < 0.041	68.56 ± 0.48 68.90 ± 0.51	0.808 ± 0.011 0.804 ± 0.011	0.299 ± 0.006 0.296 ± 0.006

mainly comes from the temperature power spectrum at high multipoles ($\ell \sim 500$ – 2000) as demonstrated in Fig. 2. Primordial standard clock models [33–37] and Wiggly Whipped Inflation [24] also provide similar improvement in fit while fitting the outliers at somewhat larger scales ($\ell < 1200$ and $\ell < 1000$, respectively). We find that the A_L effect in P18TT is mimicked by the fast roll during inflation. Interestingly, at higher multipoles the physics of fast roll and of A_L have completely different out-of-phase signals in the E -mode autocorrelation spectrum. Because of the low signal-to-noise ratio, high multipole P18 data do not help in distinguishing these two types of features. Future ground-based observations, such as Simons Observatory [38], CMB-S4 [39] complemented on large angular scales by LiteBIRD [40], or cosmic variance limited CMB space proposals such as PICO [41] or CMBBHARAT [42] will be able to provide the litmus test for these beyond standard model physics, as can be seen in Fig. 2. We find marginally better results (10.7 improvement to the TP + BK18 data), with the physics of fast roll compared to the excess lensing effect (9.7 improvement [1]).

The correlations between the fast-roll and the cosmological parameters are plotted in Fig. 3. A_L extension of the baseline model is correlated with the fast roll, as discussed for the localized linear oscillations in [2]. The degeneracy between A_L and the curvature Ω_K and the tension with other datasets have been discussed in detail in [43]. The top two panels in Fig. 3 show the degeneracy between lensing

amplitude, curvature density, and the fast-roll dynamics. The fast-roll amplitude α is negatively (positively) correlated with A_L (Ω_K). We find that a fast-rolling inflaton is able to bring the $A_L = 1$ and $\Omega_K = 0$ back within the 1σ C.L. In these two plots, we have used P18TT + BK18 data and we have also fixed the nuisance parameters, optical depth, and ω to their best-fit values.

The bounds on the parameters quoted in Table I highlight the degeneracy between a few other cosmological parameters. Importantly, with the improved fit to the data, the intermediate fast roll also helps in shifting the posterior distribution of H_0 to higher values, as happens for A_L .

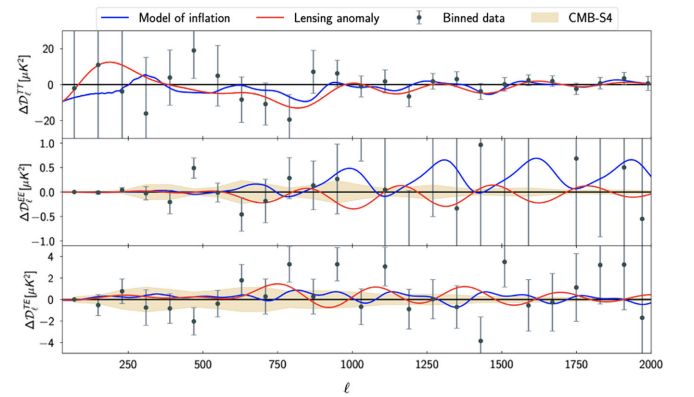


FIG. 2. The best-fit angular power spectra and Plik binned data, residual to the baseline best fit are plotted. The projected yellow error band is what we expect for CMB-S4. [39].

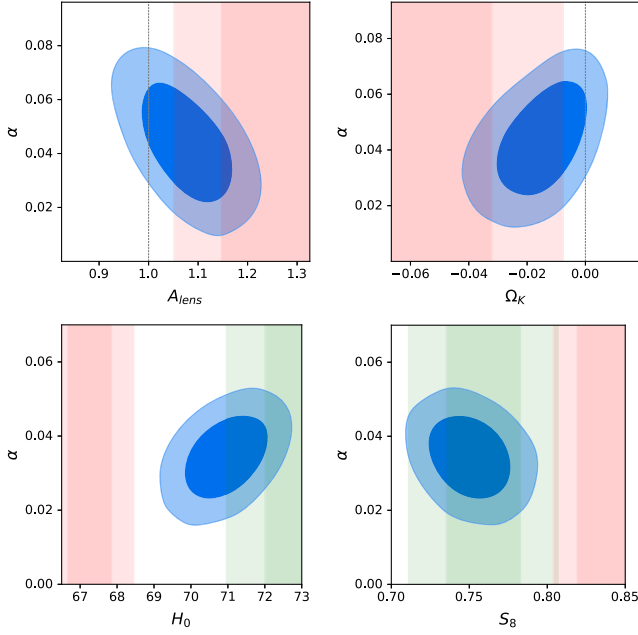


FIG. 3. Correlations between fast-roll amplitude during inflation and other cosmological parameters in P18TT + BK18 data (top) and in P18TT + BK18 + S21 (bottom). The red bands indicate the baseline bounds; the green band in the H_0 (S_8) plot indicate the constraints from SH0ES [5] (KiDS [7]). See text for more details.

For temperature data, we find a shift in the mean value of H_0 by 1.3σ with only marginal increase in the uncertainty compared to the baseline scenario. While earlier analyses [2,44] reported that certain types of features in the primordial spectrum decrease the inference of H_0 from CMB, therefore increasing the tension with the local Hubble measurements, our model, interestingly, ameliorates the tension. This decrease in the tension allows us to include H_0 prior from the recent SH0ES [5] in the analysis. For the combined datasets P18TT + BK18 + S21 and P18TP + BK18 + S21, an intermediate fast roll in the dynamics improves the fit to the data by a $\Delta\chi^2$ of 19–20 compared to the baseline. About 11 improvement in fit comes from the CMB data and nearly equal improvement is obtained from the χ^2 from SH0ES H_0 prior. The χ^2 improves as the baseline does not allow H_0 to increase without worsening the fit to the CMB data. We would like to highlight that the χ^2 from CMB in the joint P18TT + BK18 + S21 and P18TP + BK18 + S21 analyses is better than the baseline fit to the CMB-only datasets with $H_0 \sim 70$ –71. We also find that the feature parameters in the best fits for P18TT + BK18 and for P18TEEE + BK18 are different, but become very close once S21 is folded in.

In all the cases in Fig. 1 and in Table I, compared to the baseline, we find that n_s increases when we have fast-roll dynamics. With the SH0ES H_0 prior, the tilt decreases and the oscillations remain located in the same scales with

marginally higher magnitudes. Polarization and thereafter lensing addition to the temperature data restricts the shift in the tilt while keeping the oscillations largely unaltered.

The intermediate fast roll, apart from providing a *physical* solution to the A_L problem in a flat universe with a higher Hubble constant, also helps in reducing the matter density and the σ_8 normalization parameter (with direct reconstruction a numerical solution was discussed in [45,46]). A combination of these two parameters, $S_8 = \sigma_8 \sqrt{\Omega_m/0.3}$, is found to be lower than the baseline value when the inflationary dynamics has an intermediate fast-roll phase. Without any prior on the Hubble constant, we find anticorrelation between α and S_8 and a (as quoted in Table I) 1σ decrease in S_8 mean compared to the baseline value in the analysis with temperature data. This decrease makes the CMB data more compatible with the galaxy clustering and weak lensing measurements from DES [6] and KiDS [7] and brings in a new concordance. Use of the prior on H_0 further improves this agreement. This is a very interesting feature compared to other representatives of new physics discussed in the context of Hubble tension, such as early dark energy [8] or models in scalar-tensor theories of gravity [9,47,48] where S_8 increases with H_0 .

Table I provides the confidence limits for the detection of the intermediate fast roll. The highest P18TT + BK18 + S21 evidence (beyond 3σ) for fast roll is slightly decreased by polarization and lensing to 2σ .

We conclude by providing the posteriors of the HFFs and the derived potential for the scalar field, which follows from our novel methodology. Using the FGIVENX [49] package, we plot the confidence bands (Fig. 4) on the

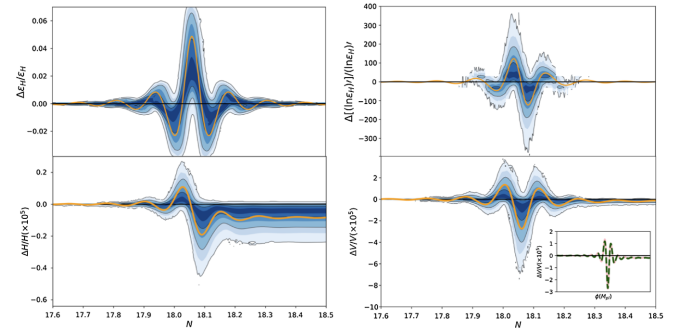


FIG. 4. Bounds on inflationary dynamics and reconstruction of the potential obtained from P18TP + BK18 + S21 combination. In the top, we plot the bounds on the fractional change in the HFFs [$\epsilon_H(N)$ and $d \ln \epsilon_H(N)/dN$] as a function of e -folds with respect to the baseline. The fractional change in the Hubble parameter (reconstructed potential) during inflation is shown in the bottom left (right). In all three plots, the inward to outward bounding lines represent $1 - 3\sigma$ confidence contours. The orange lines represent the best-fit dynamics. In the inset of the bottom right plot, we compare the fractional change in the reconstructed best-fit potential with respect to a slow-roll potential to the analytical approximation in Eq. (3).

relative difference of inflationary dynamics compared to slow roll for P18TP + BK18 + S21. The significant part of the fast-roll phase lasts for $0.5e$ -folds and the change in the Hubble parameter integrated from $\epsilon_H(N)$ can be distinguished in two parts: decaying oscillations and a step function. Therefore, when the potential is reconstructed using $V(\phi[N]) = 3M_{\text{Pl}}^2 H[N]^2 (1 - \epsilon_H[N]/3)$, we find these two features in the inflationary potential. Being agnostic about the baseline potential, we compare the numerically evaluated potential from the HFFs with the closely matching analytical approximation,

$$\frac{\Delta V(\phi)}{V_{\text{baseline}}(\phi)} = \frac{\alpha \cos[\omega(\phi - \phi_0)]}{1 + \beta(\phi - \phi_0)^2}. \quad (3)$$

Conclusions.—In this Letter, we have provided templates in the HFF during inflation leading to primordial features that mimic the effect of A_L in the P18 data. We summarize our findings below. (1) An intermediate fast roll in the inflationary dynamics for a period of $0.5e$ -folds is able to solve the lensing anomaly in a flat universe. This fast roll has a completely different signature in the polarization anisotropy spectrum compared to A_L , which can be distinguished by more precise future CMB polarization measurements at high multipoles. (2) This intermediate fast roll provides nearly 11 improvement in fit compared to the standard baseline model when compared with Planck and BICEP-Keck 2018 data. Most of the improvement (more than 8) comes from temperature data. (3) Importantly, this fast-roll model simultaneously prefers a higher value of H_0 and lower value of S_8 (only with CMB) and matter density, which brings the CMB closer to the local Hubble measurements and galaxy weak lensing measurements. When priors on the Hubble parameter are used with CMB, we find up to more than 3σ significance. With better agreement to both CMB and SH0ES data, our model provides nearly 20 improvement in fit compared to baseline. (4) A reconstruction of inflaton features in the potential from the HFF indicates the data suggested damped oscillatory modification to slow roll.

The intermediate fast-roll phase also imprints signals in the large scale structure, as studied for other types of primordial features [22,50,51]. The characteristic frequency of the superimposed oscillations can be detected in galaxy correlation function or power spectrum with the ongoing and upcoming surveys such as DESI [52], LSST [53], and Euclid [54].

The authors acknowledge the use of computational resources at the Institute of Mathematical Science’s High Performance Computing facility (Nandadevi). D. K. H. would like to thank Matteo Braglia and Xingang Chen for important discussions. A. A., F. F., and D. K. H. acknowledge travel support through the India-Italy mobility program RELIC—INT/Italy/P-39/2022(ER). F. F. acknowledges partial financial support from the

Contract by Agreement No. 2020-HH.0 ASI-UniRM2 “Partecipazione italiana alla fase A della missione LiteBIRD” and ASI/INAF for the Euclid mission n. 2018-23-HH.0. A. S. would like to acknowledge the support by National Research Foundation of Korea NRF-2021M3F7A1082053 and the support of the Korea Institute for Advanced Study (KIAS) Grant funded by the Government of Korea. D. K. H. is supported by CEFIPRA Grant No. 6704-1.

*akhilantony@imsc.res.in

†fabio.finelli@inaf.it

‡dhiraj@imsc.res.in

§shafieloo@kasi.re.kr

- [1] N. Aghanim *et al.* (Planck Collaboration), *Astron. Astrophys.* **641**, A6 (2020); **652**, C4(E) (2021).
- [2] Y. Akrami *et al.* (Planck Collaboration), *Astron. Astrophys.* **641**, A10 (2020).
- [3] D. K. Hazra, A. Shafieloo, and T. Souradeep, *J. Cosmol. Astropart. Phys.* **11** (2014) 011.
- [4] D. K. Hazra, A. Antony, and A. Shafieloo, *J. Cosmol. Astropart. Phys.* **08** (2022) 063.
- [5] A. G. Riess *et al.*, *Astrophys. J. Lett.* **934**, L7 (2021).
- [6] L. F. Secco *et al.* (DES Collaboration), *Phys. Rev. D* **105**, 023515 (2021).
- [7] M. Asgari *et al.* (KiDS Collaboration), *Astron. Astrophys.* **645**, A104 (2021).
- [8] V. Poulin, T. L. Smith, T. Karwal, and M. Kamionkowski, *Phys. Rev. Lett.* **122**, 221301 (2019).
- [9] M. Rossi, M. Ballardini, M. Braglia, F. Finelli, D. Paoletti, A. A. Starobinsky, and C. Umiltà, *Phys. Rev. D* **100**, 103524 (2019).
- [10] E. Di Valentino *et al.*, *Astropart. Phys.* **131**, 102605 (2021).
- [11] N. Schöneberg, G. Franco Abellán, A. Pérez Sánchez, S. J. Witte, V. Poulin, and J. Lesgourgues, *Phys. Rep.* **984**, 1 (2021).
- [12] F. Finelli, J. Hamann, S. M. Leach, and J. Lesgourgues, *J. Cosmol. Astropart. Phys.* **04** (2010) 011.
- [13] P. A. R. Ade *et al.* (Planck Collaboration), *Astron. Astrophys.* **571**, A22 (2014).
- [14] X. Chen, R. Easther, and E. A. Lim, *J. Cosmol. Astropart. Phys.* **04** (2008) 010.
- [15] R. Flauger, L. McAllister, E. Pajer, A. Westphal, and G. Xu, *J. Cosmol. Astropart. Phys.* **06** (2010) 009.
- [16] X. Chen, *J. Cosmol. Astropart. Phys.* **12** (2010) 003.
- [17] M. Aich, D. K. Hazra, L. Sriramkumar, and T. Souradeep, *Phys. Rev. D* **87**, 083526 (2013).
- [18] J. A. Adams, B. Cresswell, and R. Easther, *Phys. Rev. D* **64**, 123514 (2001).
- [19] D. K. Hazra, M. Aich, R. K. Jain, L. Sriramkumar, and T. Souradeep, *J. Cosmol. Astropart. Phys.* **10** (2010) 008.
- [20] D. K. Hazra, A. Shafieloo, G. F. Smoot, and A. A. Starobinsky, *J. Cosmol. Astropart. Phys.* **08** (2014) 048.
- [21] J. Chluba, J. Hamann, and S. P. Patil, *Int. J. Mod. Phys. D* **24**, 1530023 (2015).

- [22] M. Ballardini, F. Finelli, C. Fedeli, and L. Moscardini, *J. Cosmol. Astropart. Phys.* **10** (2016) 041; **04** (2018) E01.
- [23] D. K. Hazra, D. Paoletti, M. Ballardini, F. Finelli, A. Shafieloo, G. F. Smoot, and A. A. Starobinsky, *J. Cosmol. Astropart. Phys.* **02** (2018) 017.
- [24] D. K. Hazra, D. Paoletti, I. Debono, A. Shafieloo, G. F. Smoot, and A. A. Starobinsky, *J. Cosmol. Astropart. Phys.* **12** (2021) 038.
- [25] A. Antony and S. Jain, *Eur. Phys. J. C* **82**, 687 (2022).
- [26] A. Antony, F. Finelli, D. K. Hazra, and A. Shafieloo (to be published).
- [27] D. K. Hazra, L. Sriramkumar, and J. Martin, *J. Cosmol. Astropart. Phys.* **05** (2013) 026.
- [28] A. Lewis, A. Challinor, and A. Lasenby, *Astrophys. J.* **538**, 473 (2000).
- [29] A. Lewis and S. Bridle, *Phys. Rev. D* **66**, 103511 (2002).
- [30] N. Aghanim *et al.* (Planck Collaboration), *Astron. Astrophys.* **641**, A5 (2020).
- [31] P. A. R. Ade *et al.* (BICEP, Keck Collaborations), *Phys. Rev. Lett.* **127**, 151301 (2021).
- [32] M. Powell, Department of Applied Mathematics and Theoretical Physics, Centre for Mathematical Sciences, Technical Report 2009/NA06, 2009.
- [33] X. Chen, *J. Cosmol. Astropart. Phys.* **01** (2012) 038.
- [34] X. Chen, M. H. Namjoo, and Y. Wang, *J. Cosmol. Astropart. Phys.* **02** (2015) 027.
- [35] M. Braglia, X. Chen, and D. K. Hazra, *J. Cosmol. Astropart. Phys.* **06** (2021) 005.
- [36] M. Braglia, X. Chen, and D. K. Hazra, *Eur. Phys. J. C* **82**, 498 (2022).
- [37] M. Braglia, X. Chen, and D. K. Hazra, *Phys. Rev. D* **105**, 103523 (2021).
- [38] P. Ade *et al.* (Simons Observatory Collaboration), *J. Cosmol. Astropart. Phys.* **02** (2019) 056.
- [39] K. Abazajian *et al.*, arXiv:1907.04473.
- [40] E. Allys *et al.* (LiteBIRD Collaboration), *Prog. Theor. Exp. Phys.* (2022).
- [41] S. Hanany *et al.* (NASA PICO Collaboration), arXiv:1902.10541.
- [42] <http://cmb-bharat.in>.
- [43] E. Di Valentino, A. Melchiorri, and J. Silk, *Nat. Astron.* **4**, 196 (2019).
- [44] M. Liu and Z. Huang, *Astrophys. J.* **897**, 166 (2020).
- [45] D. K. Hazra, A. Shafieloo, and T. Souradeep, *J. Cosmol. Astropart. Phys.* **04** (2019) 036.
- [46] R. E. Keeley, A. Shafieloo, D. K. Hazra, and T. Souradeep, *J. Cosmol. Astropart. Phys.* **09** (2020) 055.
- [47] M. Ballardini, M. Braglia, F. Finelli, D. Paoletti, A. A. Starobinsky, and C. Umiltà, *J. Cosmol. Astropart. Phys.* **10** (2020) 044.
- [48] M. Braglia, M. Ballardini, F. Finelli, and K. Koyama, *Phys. Rev. D* **103**, 043528 (2021).
- [49] W. Handley, *J. Open Source Software* **3**, 849 (2018).
- [50] D. K. Hazra, *J. Cosmol. Astropart. Phys.* **03** (2013) 003.
- [51] M. Ballardini, R. Murgia, M. Baldi, F. Finelli, and M. Viel, *J. Cosmol. Astropart. Phys.* **04** (2020) 030.
- [52] DESI Collaboration, arXiv:1611.00036.
- [53] Ž. Ivezić *et al.* (LSST Collaboration), *Astrophys. J.* **873**, 111 (2019).
- [54] G. D. Racca *et al.*, *Proc. SPIE Int. Soc. Opt. Eng.* **9904**, 00 (2016).